

# Synthesis of Carbon black/geopolymer composites with high and stable electrothermal performance

Sibtt Mohammed Jabbar, Dalya Hekmat Hameed, and Imad Ali Disher\*

Department of Ceramics and Building Materials, College of Materials Engineering, University of Babylon, Babil, Iraq.

\*Corresponding Author:

E-mail Address: [imadali4@uobabylon.edu.iq](mailto:imadali4@uobabylon.edu.iq)

## Abstract

Geopolymer/nano carbon black composite is a promising electrically conductive smart material that can be used in self-heating and self-sensing applications. This paper studies the effect of adding nano carbon black to the physical, mechanical, electrical, and electrothermal performance of metakaolin-based geopolymer. Carbon black was added at the percent of 5%, 10%, 15%, and 20% by weight of metakaolin; the compressive strength was tested at various ages of 7, 14, 28, and 90 days, and the electrothermal performance was tested using AC and DC voltages. The results showed that a compromise between suitable compressive strength and high electrothermal conversion could be achieved when a specific balance between the carbon black percent and the lowest water content is established. A composite with a compressive strength of 27 MPa and stable electrothermal performance reaching 142°C at 9V DC can be prepared using 20 wt% of carbon black and a water-to-metakaolin ratio of 0.549, which is used as a smart material in construction applications.

**Keywords:** Geopolymer, Nano carbon black, Metakaolin, Electrothermal, Self-heating, Smart materials.

## 24 1. Introduction

25 Geopolymer is a promising alternative to ordinary Portland cement, which is a traditional building  
26 material [1]. It is characterized by its resistance to high temperature and corrosion [2,3], high  
27 mechanical performance and high durability [4–6]. Also, it is an environmentally friendly material  
28 due to the low emission of CO<sub>2</sub> gas from its production processes [7,8]. Because of its unique  
29 properties, geopolymer can be used in construction applications as well as in many other  
30 applications, such as heavy metal immobilization [9–11], coating applications [12], and fire  
31 resistance applications [13].

32 Geopolymer is manufactured from raw materials rich in alumina and silica after mixing with an  
33 alkaline solution. Geopolymer materials are generally formed by three types of polysialate 3D  
34 networks consisting of SiO<sub>4</sub> and AlO<sub>4</sub> tetrahedrons, which are polysialate (-Si-O-Al-O-),  
35 polysialate-siloxo (-Si-O-Al-O-Si-O-) and polysialate-disiloxo (-Si-O-Al-O-Si-O-Si-O-). The  
36 cavities within these networks are filled by corresponding cations (Na<sup>+</sup>, K<sup>+</sup>, Ca<sup>++</sup>, and Cs<sup>+</sup>)  
37 contributing to balancing the negative charge for Al<sup>+3</sup> [14]. The performance of geopolymer  
38 depends mainly on the properties of its raw materials; metakaolin is considered one of the best  
39 precursors for manufacturing geopolymer due to its high fraction of silica and alumina, low  
40 impurities, stable chemical composition, and high purity compared to fly ash and slag [15–17].

41 Carbon black is a substance that is difficult to dispose of and is produced from various industrial  
42 processes as byproducts, in the form of a fine powder containing a high percentage of carbon; it is  
43 characterized by high specific surface area, high chemical and thermal stability, and good electrical  
44 conductivity, also this waste is usually decomposed into landfills causing soil contamination and  
45 water pollution [18].

46 Geopolymer is not electrically conductive in its dry state, so carbon black can be added to improve  
47 its electrical conductivity, and thus, it becomes a material that can be used in self-heating [19] and

48 self-sensing [20] applications. Carbon black cannot be added in high proportions due to the  
49 negative effect on the mechanical properties [19,21,22].

50 Many studies have dealt with adding carbon black to improve the electric performance of  
51 geopolymers. Arif et al. made a composite material from geopolymer with the inclusion of carbon  
52 black to be used as an X-ray shield [23]. Rauf et al. added carbon black with  $\text{Fe}_3\text{O}_4$  to improve the  
53 electrical and optical properties and gamma ray absorption of the geopolymer [24]. Gu et al. added  
54 nanocarbon black with carbon fibers to improve the electrothermal performance of geopolymers  
55 used in paving Airports [25]. Han et al. found that adding 15 vol% and 0.05 vol% of both nano  
56 carbon black and carbon fibers to the geopolymer gives the best result in terms of electrical  
57 conductivity [26]. Mizerová et al. studied the effect of adding carbon black, at a percentage not  
58 exceeding 2% by weight of fly ash, on the self-sensing property of geopolymer [27]. Irshidat et  
59 al. studied the effect of adding carbon black at percentages of 5%-40% by weight of fly ash on the  
60 mechanical and physical properties of geopolymer; they found that adding carbon black at 5% and  
61 20% leads to an increase in compressive strength to 46.89 and 45.9 MPa, respectively, compared  
62 to the compressive strength of the reference sample at 44.79 MPa [18]. Cai et al. studied the effect  
63 of self-heating on accelerating the curing of geopolymer by adding carbon black and steel fibers  
64 at 6 and 2 vol%, respectively; they obtained a sample with the unstable electrothermal performance  
65 of 67°C at 110 DC Volts [28]. Fiala et al. studied the effect of adding carbon black to geopolymer,  
66 at 2.25% by weight of slag, on the physical, mechanical, thermal, and electrical properties by  
67 applying 40 and 100 DC volts; they obtained samples with compressive strength of 7.31 MPa,  
68 electric conductivity of  $1.3 \times 10^{-1}$  S/m, and electrothermal performance of 44°C, 125°C at 40, 110  
69 DC volts, respectively [19].

70 The mechanical strength of the pristine geopolymer utilized in some of these studies is already low,  
71 as reported in [21,22] is due to the fact that the materials utilized are not really a geopolymer, based  
72 on the precise definition of the geopolymer given by Joseph Davidovits [14], but they are alkali-

73 activated materials mistakenly called geopolymers, as many researchers use the two terms as  
74 synonyms. Also, the electrothermal performance reported in these studies is noticeably weak as a  
75 high voltage is required to produce low temperature, as reported in [19,28]. Moreover, the stability  
76 of the electrothermal performance of the self-heating composites isn't reported in the literature.

77 It is well known that the geopolymer with a well-defined composition and structure has mechanical  
78 strength higher than that of the alkali-activated materials [29]. Thus, if the geopolymer is prepared  
79 with the right composition, it is expected that a suitable percent of carbon black can be incorporated  
80 into it while maintaining acceptable mechanical strength for structural applications. Hence, a high  
81 electrothermal performance can be achieved.

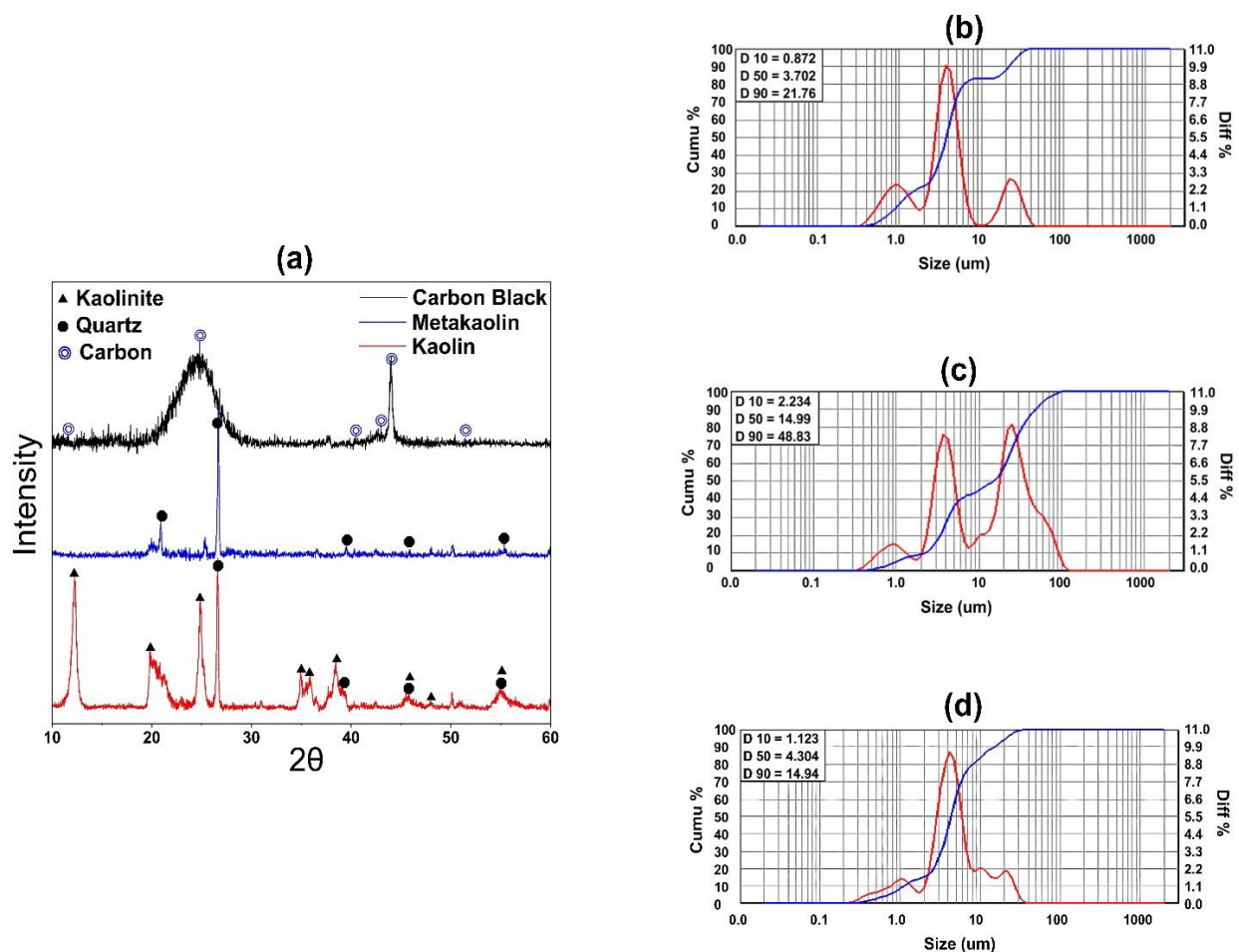
82 The current study investigates the effect of adding nano carbon black on the electrothermal  
83 performance of metakaolin-based geopolymer as well as its mechanical, physical, and electrical  
84 properties. Carbon black was added at a weight percent of 5%, 10%, 15%, and 20%, with respect  
85 to the metakaolin content, and the compressive strength was measured at various ages of 7, 14, 28,  
86 and 90 days. The electrothermal performance was tested using AC and DC voltages up to 12 V,  
87 and the stability of this performance was also assessed.

## 88 **2. Materials and Methodology**

### 89 **2.1. Materials**

90 Metakaolin ( $\text{SiO}_2$  w.t%= 54.46,  $\text{Al}_2\text{O}_3$  w.t%= 33.68,  $\text{Na}_2\text{O}$  w.t%= 0.22), nano carbon black powder  
91 (N330, RPSG Group - India), industrial sodium hydroxide flakes (99% purity, from Al-Kout  
92 Company - Kuwait), industrial sodium silicate solution ( $\text{Na}_2\text{O}$  w.t% = 13.1-13.7,  $\text{SiO}_2$  w.t%= 32-  
93 33, United Arab Emirates), copper tape with a width of 21 mm and a thickness of 0.1 mm used as  
94 electrodes, and laboratory distilled water are the materials used for producing conductive  
95 geopolymer samples. Metakaolin was produced from the calcination of kaolin (Supplied by Al-  
96 Mishraq Company - Iraq) at a temperature of 800°C for three hours. **Figure 1(a)** shows the XRD

97 patterns of the kaolin, metakaolin, and carbon black; the diffraction data are in good agreement  
 98 with the JCPDS cards (00-001-0527), (00-033-1161), and (01-074-2330) of the kaolinite, quartz,  
 99 and carbon respectively.  $D_{50}$  for the kaolin, metakaolin, and carbon black is (3.702, 14.99, and  
 100 4.304)  $\mu\text{m}$ , respectively, as can be seen in **Figure 1(b, c, d)**.



101  
 102 **FIGURE 1** (a) XRD patterns of the kaolin, metakaolin, and carbon black; and the particle size  
 103 distribution of the (b) kaolin, (c) metakaolin, and (d) carbon black

104  
 105 **2.2. Methodology**

106 **2.2.1. Samples Preparation**

107 **Table 1** presents the weights of metakaolin (MK), carbon black-to-metakaolin ratio (CB/MK),  
 108 sodium silicate-to-metakaolin ratio (SS/MK), sodium hydroxide-to-metakaolin ratio (SH/MK),  
 109 and the water-to-metakaolin ratio (W/MK) used in the sample preparations for this study. For these

110 samples, the geopolymer has the formula  $\text{Na}_2\text{O} \cdot \text{Al}_2\text{O}_3 \cdot 3.6\text{SiO}_2$ , which was optimized in our  
111 previous work to have a compressive strength of 117 MPa [30].

112 **TABLE 1** Samples ID and the composition of the samples

Sample ID	MK (g)	CB/MK	SS/MK	SH/MK	W/MK
GP-0	120.812	0	0.9755	0.0934	0.116
GP-1A	90.609	0.05	0.9755	0.0934	0.549
GP-1B	90.609	0.05	0.9755	0.0934	0.632
GP-1C	90.609	0.05	0.9755	0.0934	0.715
GP-2A	90.609	0.1	0.9755	0.0934	0.549
GP-2B	90.609	0.1	0.9755	0.0934	0.632
GP-2C	90.609	0.1	0.9755	0.0934	0.715
GP-3A	90.609	0.15	0.9755	0.0934	0.549
GP-3B	90.609	0.15	0.9755	0.0934	0.632
GP-3C	90.609	0.15	0.9755	0.0934	0.715
GP-4A	90.609	0.2	0.9755	0.0934	0.549
GP-4B	90.609	0.2	0.9755	0.0934	0.632
GP-4C	90.609	0.2	0.9755	0.0934	0.715

113  
114 Sodium hydroxide (99% purity, Al-Kout Co. - Kuwait) solution was prepared by dissolving  
115 sodium hydroxide flakes in 10 ml of laboratory distilled water, the desired amount of the sodium  
116 silicate solution was added to the sodium hydroxide solution, and the solution was heated up to  
117  $82 \pm 2^\circ\text{C}$  for 15 minutes, under stirring at a speed of 750 rpm, and it was left to cool before use.

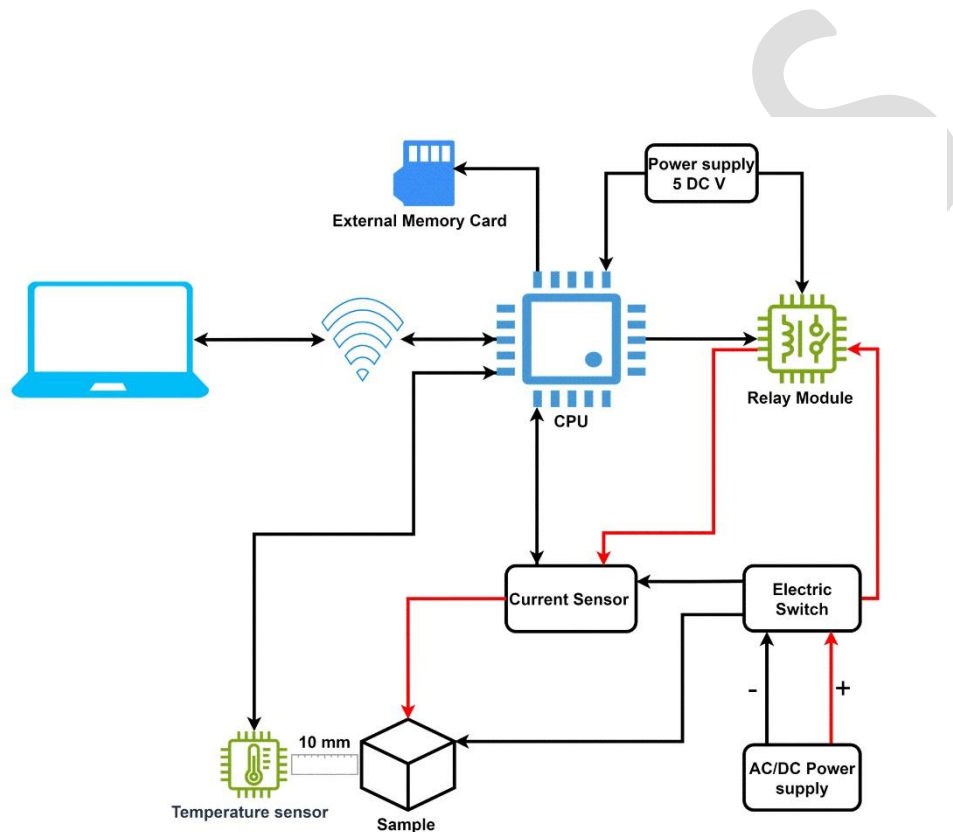
118 Carbon black (Industrial grade, N330, RPSG Group - India) powder was added to the solution  
119 resulting from the previous step and mixed for 2 minutes at a speed of 700 rpm using an electronic  
120 overhead stirrer (SL3000D - global lab. co). During mixing, water is added according to the  
121 composition given in **Table 1**, excluding the 10 ml used to prepare the sodium hydroxide solution.  
122 After that, the metakaolin powder was mixed with the mixture resulting from the previous step at

123 a speed of 3000 rpm for 5 minutes. The paste resulting from the previous step was poured into  
124 molds made of silicone rubber, which are of three types: cylindrical molds with dimensions of  
125 23x46 mm for testing compression strength, cubic molds with dimensions of 20x20x20 mm  
126 containing two longitudinal slots on opposite sides, separated by 8 mm to fix copper electrodes,  
127 used to investigating the electrical properties and electrothermal performance, and rectangular molds  
128 with dimensions of 20x20x6 used for testing the physical properties and SEM examination. The  
129 copper electrodes were installed after pouring the paste into the molds through the mold slots. The  
130 samples were demolded after 72 hours and kept in the laboratory atmosphere at a temperature of  
131  $18\pm 2^{\circ}\text{C}$  and relative humidity of 50% until the tests; all tests were conducted 28 days after  
132 demolding the samples except the compression strength test, which is performed at different ages  
133 of 7, 14, 28, and 90 days.

### 134 2.2.2. Characterization

135 The bulk density, true density, apparent porosity, and water absorption of the samples were tested  
136 according to Archimedes' principle. An Impact-Automatic Console-2000 KN machine was used  
137 to test the compressive strength of samples. SEM examination was used to investigate the  
138 microstructural features of the samples using TESCAN- VEG 3 SBU nanospace machine. Hioki  
139 IM 3536 device was used to measure impedance ( $Z$ ), phase angle ( $\theta$ ), and electrical resistance  
140 ( $R_{dc}$ ). The EIS Spectrum Analysis software was also used to analyze the results and determine the  
141 equivalent electrical circuit for the spectrum of the tested samples by using the NM Simp algorithm  
142 and the Amplitude function. A direct and alternating voltage was applied to study the  
143 electrothermal performance of the geopolymer/carbon black samples. A device consisting of a  
144 processing unit board connected to a sensor for measuring current, a sensor for measuring the  
145 surface temperature of the sample, and an AC/DC power supply, was used to detect the surface  
146 temperature of the sample and the consumed current when a given voltage is applied. **Figure 2**

147 shows the test device schematic. The operation of the device is controlled via a computer, which  
148 provides simultaneous measurement of current and temperature. The test voltage was selected  
149 based on the electrical resistance of the samples. To avoid overheating, all samples were tested at  
150 12 volts, with the exception of GP-4A, which was tested at 9 volts. A quick test with a single  
151 heating cycle, 2 h of heating, and 0.5 an hour of cooling was conducted for all samples to determine  
152 the electrothermal performance. Subsequently, selected samples were chosen and tested over three  
153 cycles.



154  
155 **FIGURE 2** A schematic of the test device

### 156 3. Results and Discussions

#### 157 3.1. Physical Properties (Bulk and True density, apparent porosity, water absorption)

158 **Table 2** shows the values of the bulk density, true density, apparent porosity, and water absorption  
159 of the samples; it can be noted that the geopolymer samples have higher density compared to the  
160 composite samples that contain an additional percentage of carbon black. This is consistent with

161 studies showing that the incorporation of conductive filler can increase the porosity and reduce the  
 162 bulk density of composite materials. While the relatively low density of carbon black may partially  
 163 contribute to this effect, the increase in porosity is mainly attributed to its hydrophobic nature and  
 164 the way it interacts with the binder matrix, and as the percentage of conductive filler increases, the  
 165 pore size increases [31,32]. Also, it can be attributed to the low density of the carbon black as  
 166 compared to the geopolymer, as well as the amount of water used to utilize the preparation of the  
 167 composites seems to affect the density; part of this water is necessary to wet the carbon black and,  
 168 hence, facilitate the preparation process while the residual amount of that water leads to the  
 169 formation of more pores and, hence, lower bulk density. Also, this water works on impeding the  
 170 polymerization process leading to lower true density for the geopolymer [33]. It can be noticed  
 171 that the sample GP-3B has a lower porosity among the composites, indicating that it contains a  
 172 lower amount of residual water. This is consistent with the study that shows that harmonizing the  
 173 water / solid fraction leads to improving density [34].

174 **TABLE 2** The bulk density, true density, apparent porosity, and water absorption of the  
 175 samples

Sample ID	Bulk density (g/cm <sup>3</sup> )	True density (g/cm <sup>3</sup> )	Apparent porosity (%)	Water absorption (%)
GP-0	1.5351	2.3495	34.6	22.5
GP-1A	1.2276	2.2208	44.7	36.4
GP-1B	1.1645	2.3177	49.7	42.7
GP-1C	1.1510	2.3347	50.6	44
GP-2A	1.2001	2.1531	44.2	36.8
GP-2B	1.1813	2.2250	46.9	39.7
GP-2C	1.1470	2.1855	47.5	41.4
GP-3A	1.1820	1.9343	38.8	32.9
GP-3B	1.1980	1.8673	35.8	29.9
GP-3C	1.1243	2.0628	45.4	40.4

<b>GP-4A</b>	1.1261	1.9316	41.6	37
<b>GP-4B</b>	1.1119	1.8754	40.7	36.6
<b>GP-4C</b>	1.1115	1.9835	43.9	39.5

176

177

### 178 3.2. Compressive Strength

179 **Figure 3** shows the compressive strength of geopolymer samples with different percent of carbon  
 180 black. From **Figure 3(a)**, it is evident that the compressive strength of geopolymer samples is  
 181 higher compared to those containing carbon black; this is because, in addition to the higher porosity  
 182 of the composites, the carbon black is an inert phase within the geopolymer matrix that generates  
 183 weak point via the aggregation [35], this can be clearly noticed in **Figure 3(b-e)** as the compressive  
 184 strength at the age of 90 days of samples GP-1, GP-2, GP-3, and GP-4 are reduced due to the  
 185 increase of the carbon black percent. Furthermore, there is a decrease in the compressive strength  
 186 with increased water content for these samples due to the increase of the porosity. Notably, the  
 187 samples GP-1 have the highest compressive strength among the composites due to their higher  
 188 density.

189 Additionally, it has been observed that the increase in the compressive strength over time, which  
 190 indicates the progress of the polymerization process, for GP-0 between 7 and 90 days is about  
 191 26%. For the composites, this percent varies not only with the water content, which is known to  
 192 impede the polymerization but also with the percent of the carbon black; this indicates that carbon  
 193 black affects the polymerization process; however, investigating its role in this process requires  
 194 further studies.

### 195 3.3. Scanning Electron Microscope Images

196 **Figure 4** shows the SEM images of the GP-0 sample. **Figure 4(a)** confirms the presence of a  
197 continuous phase that is formed via the polymerization process; in this phase, different forms of  
198 scraps are impeded, as appears more clearly in **Figures 4(b and c)**. This scrap can be assigned to  
199 the inert phases that can't participate in the polymerization process. **Figure 4(d)** shows the un-  
200 polished surface of the sample in which the pores and the drying microcracks are clearly appeared.  
201 **Figures 5-7** show the microstructure of the composites. The aggregation of the carbon black is  
202 observed in the composites; as the percent of the carbon black or the amount of water increases,  
203 the size of the aggregates increases. Also, the images confirm the presence of microcracks that  
204 pass through the geopolymer matrix, these cracks can be assigned to the drying of the surface of  
205 the samples [36], and it can be noticed that the cracks pass through the carbon black aggregates,  
206 **Figures 5a and 6a**, this indicates that the aggregates are weaker than the interface. Also, in the  
207 case of high percent of carbon black, **Figures 6b, c and 7b, c**, a separation between the geopolymer  
208 and the aggregates is noticed; this can be attributed to the hydrophobicity of the carbon black that  
209 led to weak interaction with hydrophilic geopolymer matrix [37,38].

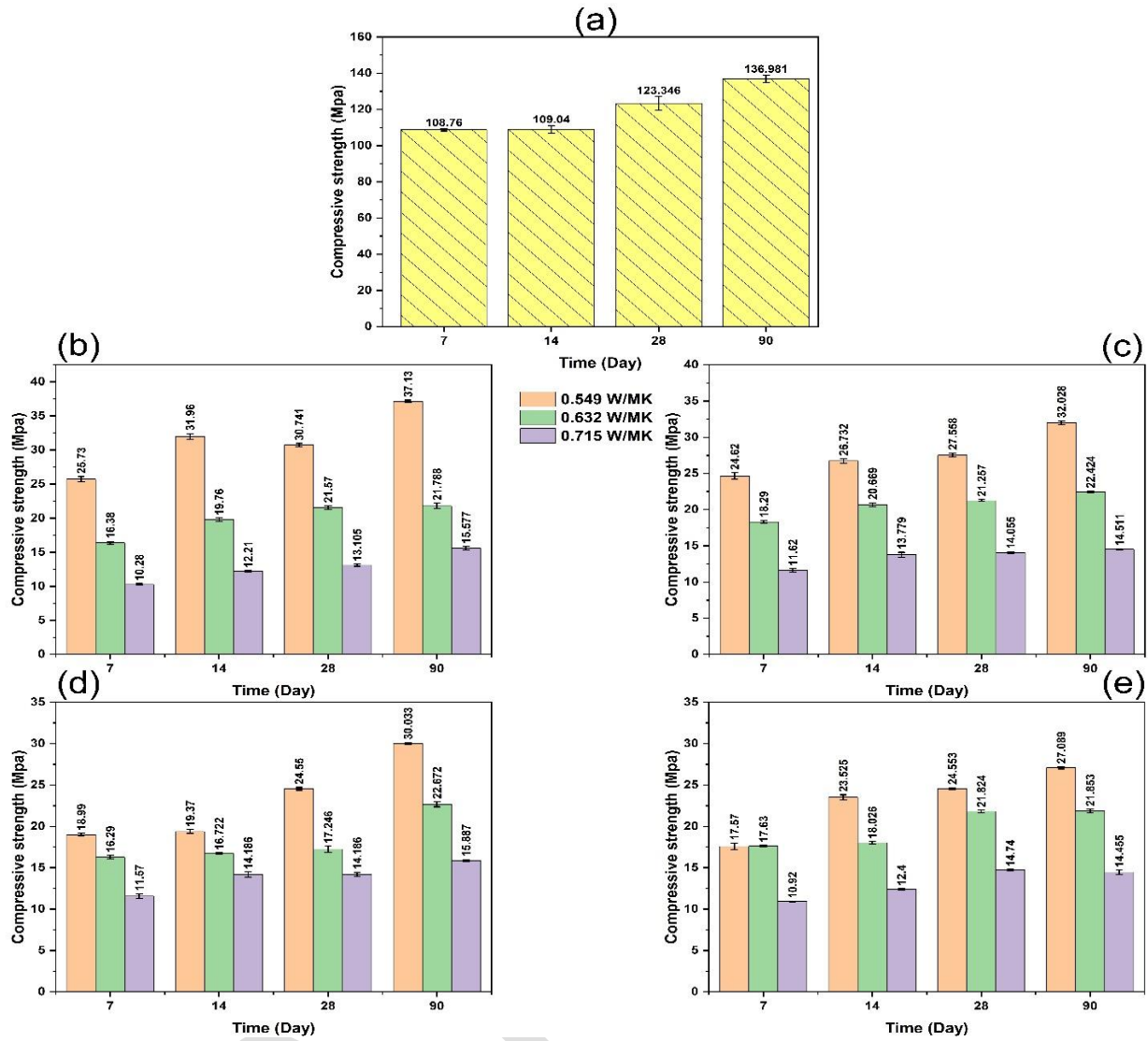


**FIGURE 3** The compressive strength of geopolymer samples (a) GP-0, (b) GP-1, (c) GP-2, (d) GP-3, and (e) GP-4

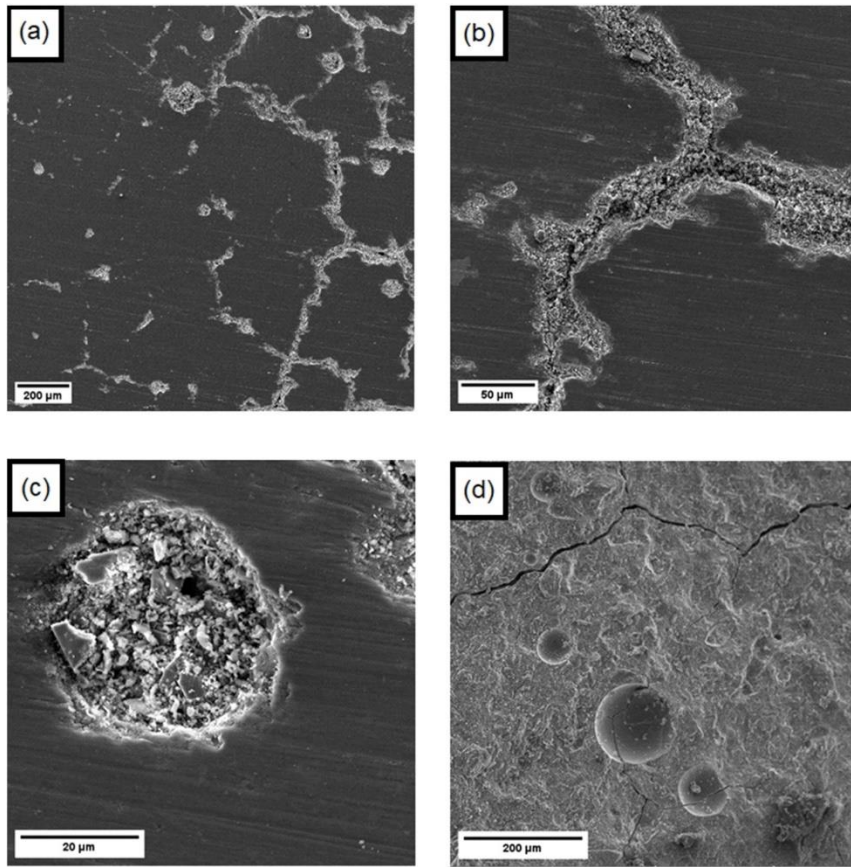
210

211

212

213

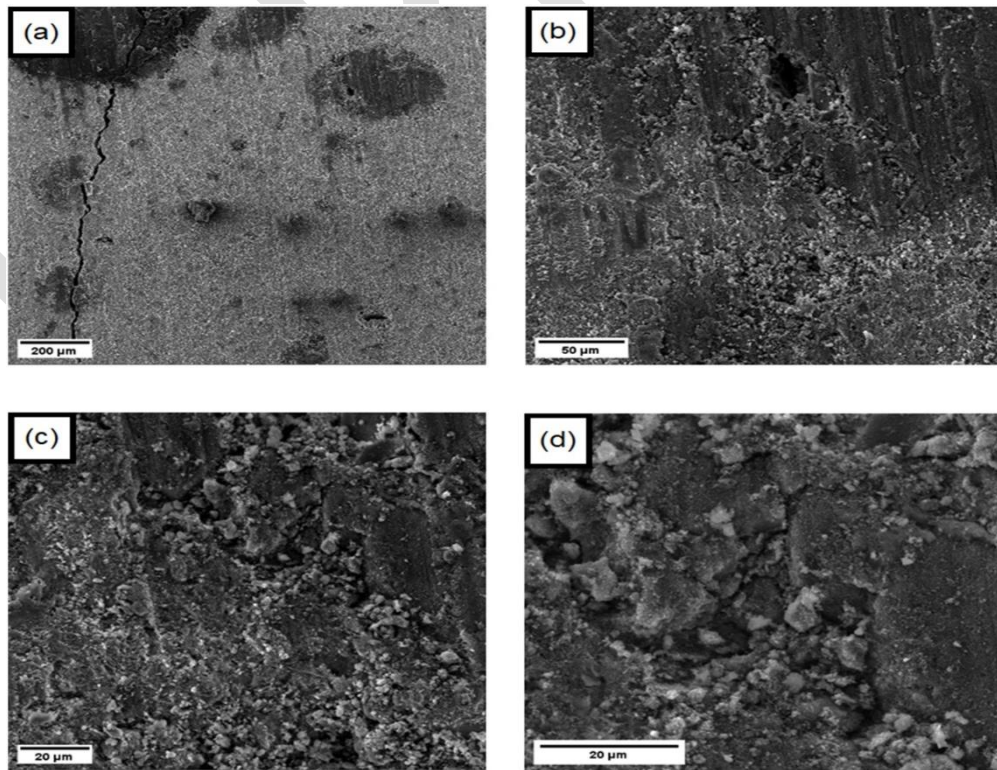
214



215

216

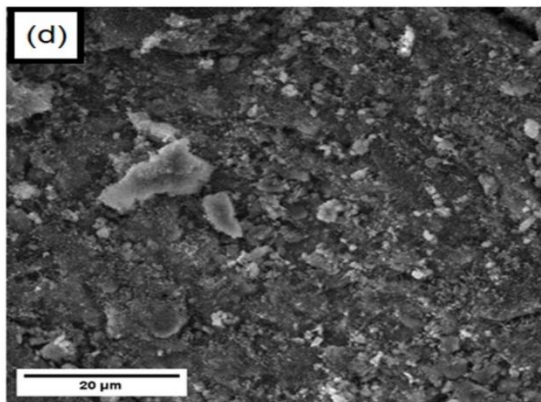
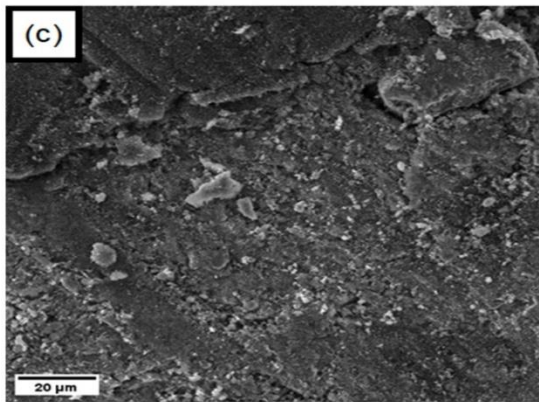
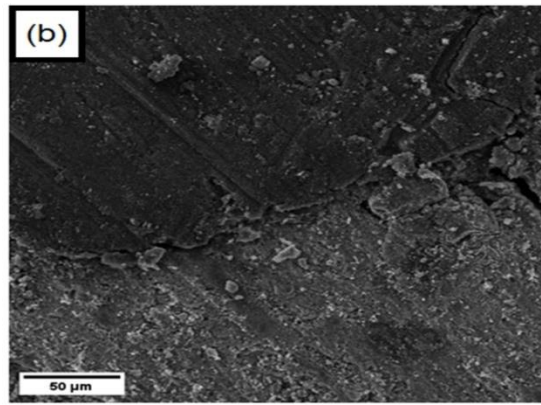
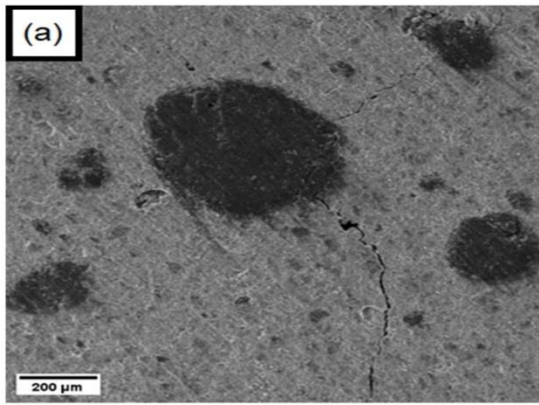
**FIGURE 4** The SEM images of sample GP-0



217

218

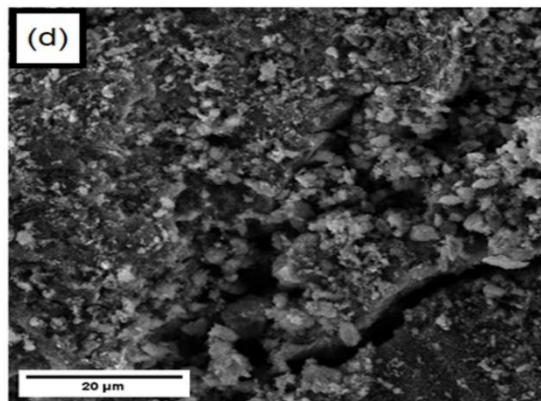
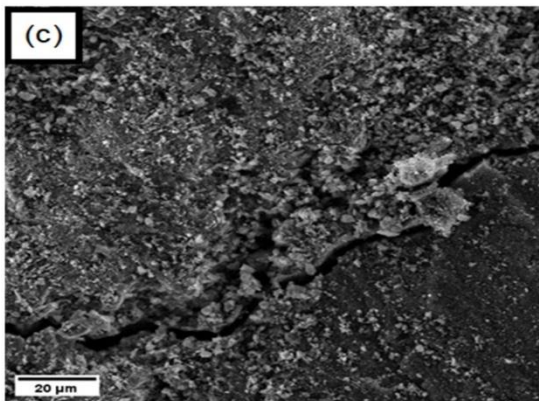
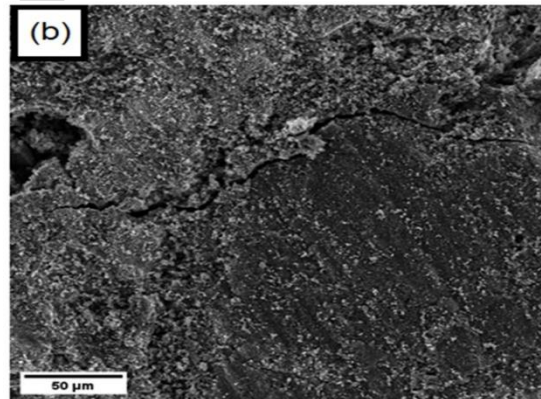
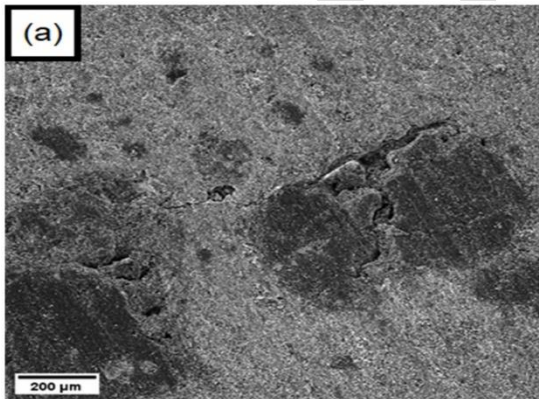
**FIGURE 5** The SEM images of sample GP-2A



219

220

**FIGURE 6** The SEM images of sample GP-2B



221

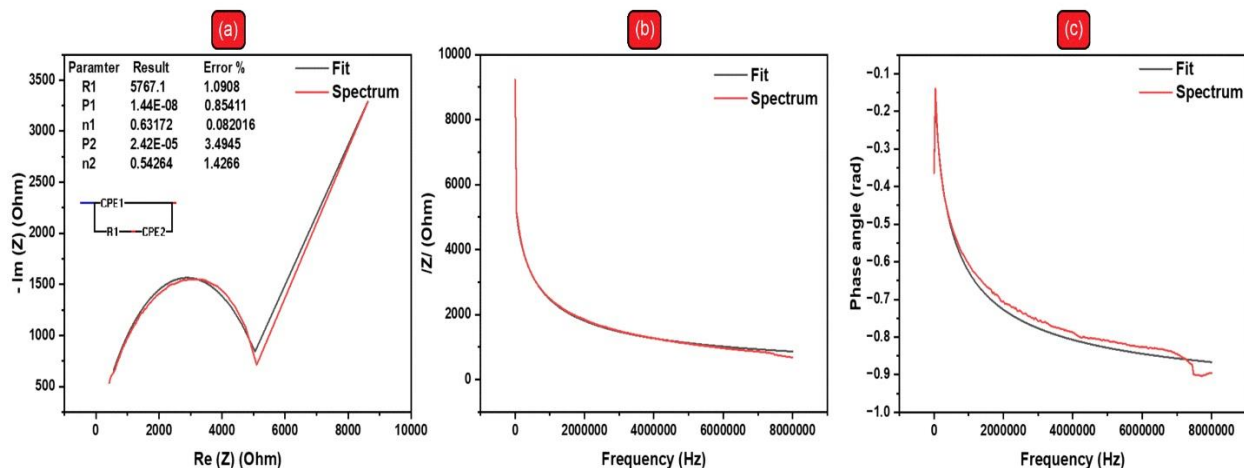
222

FIGURE 7 The SEM images of sample GP-4A

223

### 224 3.4. Electrochemical Impedance Spectroscopy

225 **Figure 8** shows the Nyquist plot, Bode plot, and the values of the phase angle for GP-0. It has  
 226 been found, using the fitting and simulation of the Nyquist plot, that the equivalent electrical circuit  
 227 that describes the geopolymer sample is  $CPE_1 / (R_1 + CPE_2)$ . This indicates that the material has a  
 228 dielectric feature. As expected, the magnitude of impedance decreases with increasing frequency.  
 229 Furthermore, the phase angle between voltage and current is negative, which is a characteristic of  
 230 materials with capacitive behavior.



231

232 **FIGURE 8** Nyquist plot (a) and (b-c) Body plot from EIS of GP-0

233

234 **Figures 9** show the Nyquist plot, Bode plot, and the values of the phase angle for geopolymer  
 235 composites with various carbon black percent. The equivalent electrical circuit that describes each  
 236 composite is given below:

- 237 • GP-1A:  $(CPE_1 / (R_1 + CPE_2 / R_2))$
- 238 • GP-1B:  $CPE_1 / (R_1 / CPE_2)$
- 239 • GP-3C:  $(R_1 / CPE_1 + (R_2 + CPE_2))$

240 • GP-4B:  $(CPE_1/R_2) + (R_1/CPE_2)$

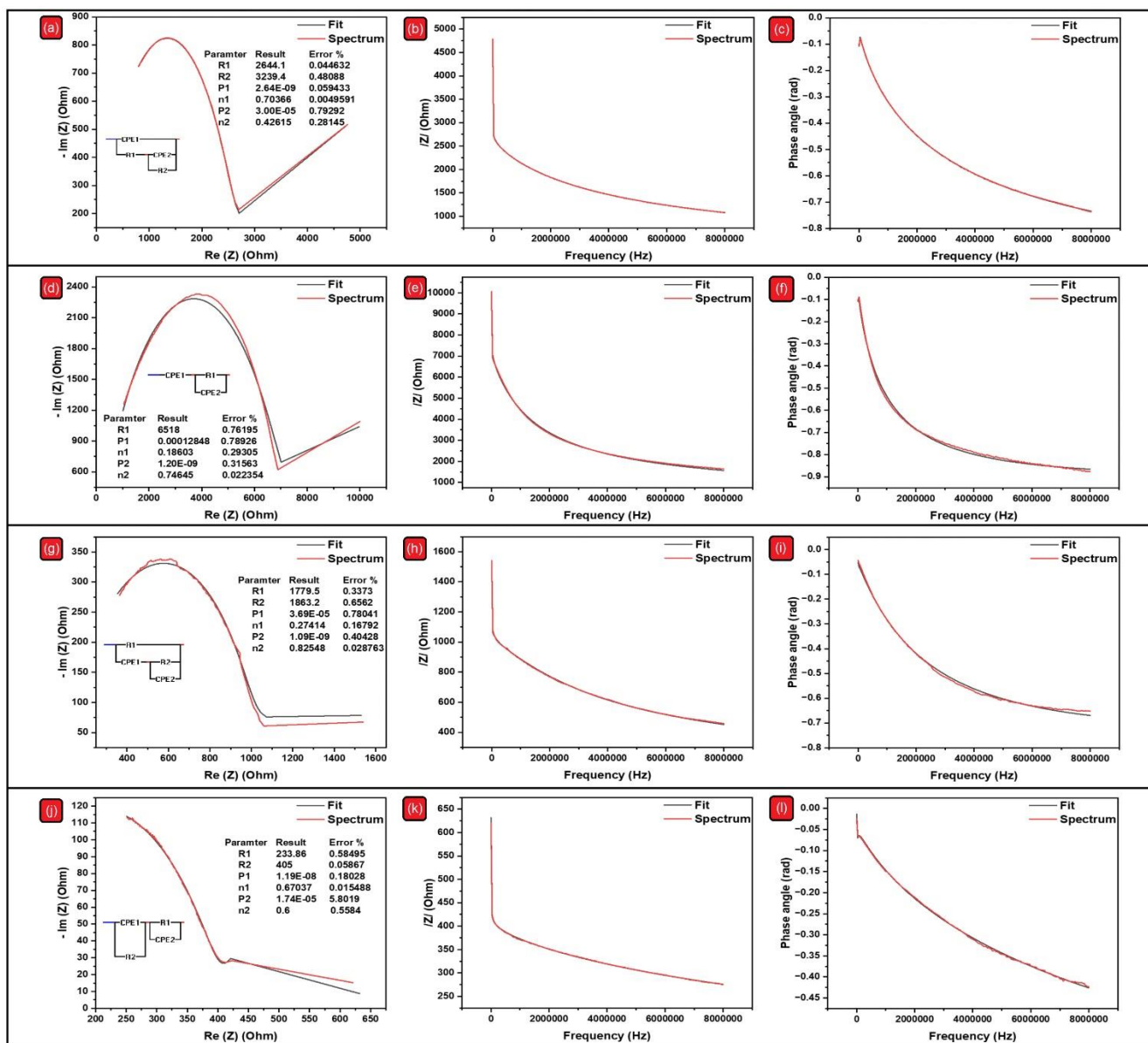
241 From the EIS results, the presence of more than one resistance in equivalent electrical circuits has  
242 been noticed; this indicates the presence of more than one process area that affects the transfer of  
243 charges. These resistances are the result of the simple ohmic resistance resulting from the flow of  
244 current through the material, the resistance of the material, the resistance to the transfer of charge  
245 from the electrode to the material, and the resistance to the diffusion of charges [39]. In addition,  
246 the presence of more than one value for the constant phase element (CPE) was noticed; this  
247 indicates the presence of electrical complexities within the material that affect the electrical  
248 behavior; the causes of these complexities are electrochemical reactions on the surfaces of the  
249 granules and the surfaces of the pores, corrosion reactions, and the presence of thin films [39].

250 It should be noted that the equivalent electrical circuit, which describes each of GP-1C, GP-2A,  
251 GP-2B, and GP-2C, is the same equivalent electrical circuit that describes the sample GP-1B.  
252 Similarly, the equivalent electrical circuit that describes each of GP-3A, GP-3B, and GP-4A is the  
253 same equivalent electrical circuit that describes sample GP-3C. The GP-4C is described by the  
254 same equivalent electrical circuit as the GP-4B. Also, it should be noted that only the values of the  
255 elements forming the equivalent electrical circuit change with changes in the addition percent and  
256 water content. This is due to the increased electrical complexities within the material resulting  
257 from changes in density and porosity [39].

258 The Bode plots for GP-1, GP-2, GP-3, and GP-4 composites showed that the impedance decreases  
259 with increasing frequency across all water content. As for the phase angle, it remains negative for  
260 all samples at all frequencies; this behavior is due to the fact that the phase angle is negative,  
261 meaning that the material has capacitive behavior.

262 3.5. Electric Resistance (R<sub>dc</sub>)

263 **Table 3** shows the electrical resistance values of geopolymer and geopolymer/carbon black  
 264 composites. It is noted that the value of electrical resistance decreases with the increase in the  
 265 percent of carbon black added; this is an expected result of the increase in conduction paths within  
 266 the material.



267 **FIGURE 9** Nyquist plots (a, d, g, j) and (b-c; e-f; h-i; k-l) Bode plots from EIS of GP-1A,  
 268 GP-1B, GP-3C, GP-4B, respectively.  
 269

270  
 271 It is also noted that the value of electrical resistance increases with increasing water content, and  
 272 this behavior is due to the increase in porosity, which is observed in all samples except for (GP-

273 2B, GP-3B, GP-4B), where there is a heterogenous distribution of additive within the samples, as  
 274 appear more clearly in **Figures 10**. The electrical resistance of the composites is the result of the  
 275 (i) formation of the conductive paths that reduce the electrical resistance, (ii) the presence of the  
 276 pores filled with carbon black, which behave as a junction that facilitates the connection between  
 277 the conductive paths, and (iii) the presence of empty pores which cut the conductive paths. The  
 278 time factor must be taken into consideration when examining electrical resistance, as its value  
 279 increases with time as a result of the loss of water that participates in the electrical conduction  
 280 process as the polymerization process continues [40], or its value decreases with the loss of water  
 281 present in the pores, and thus the conductive filler agglomerates and forms additional paths [41].

282 **TABLE 3** The values of the electrical resistance of the samples

Sample ID	Rdc ( $\Omega$ )	Sample ID	Rdc ( $\Omega$ )
GP-0	8638	GP-3A	497.655
GP-1A	4307.18	GP-3B	919.06
GP-1B	8995.58	GP-3C	1413.838
GP-1C	12508.2	GP-4A	142.009
GP-2A	2549.53	GP-4B	535.039
GP-2B	8657.59	GP-4C	675.497
GP-2C	4060.5		

283

284

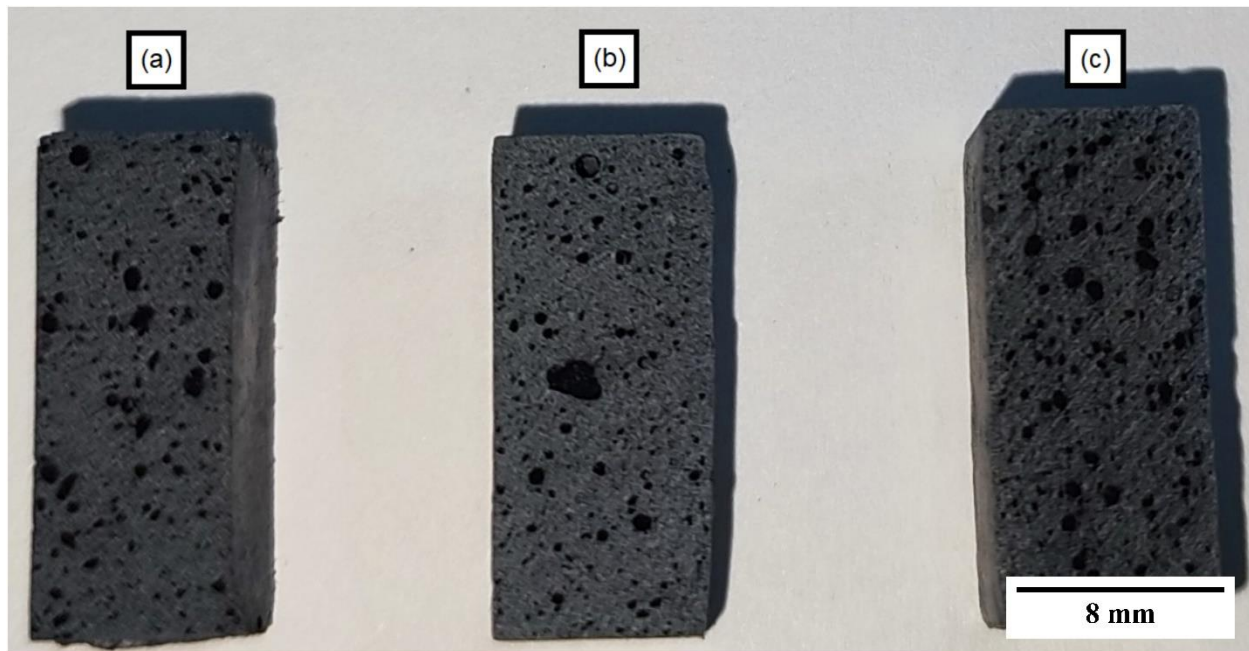


**FIGURE 10** Distribution of carbon black (a) GP-2A, (b) GP-2B, (c) GP-2C

### 3.6. Electrothermal Performance

Due to the high electrical resistance of the GP-0, its electrothermal effect hasn't a practical value.

**Figure 11** shows the electrothermal effect of the geopolymer composites tested over a single

heating cycle of two hours and a cooling period of half an hour, with both AC and DC voltages. It

has been found that GP-1 samples can reach a temperature of around 32.75°C, GP-2 samples

achieve a temperature of 32-34°C, GP-3 samples reach a temperature of 34-44°C, and GP-4

samples achieve a temperature of 37-50°C by an applied voltage of 12 volts, with the exception of

GP-4A sample that reaches to a temperature of 62°C by an applied voltage of 9 volts. It has been

observed that the electrothermal effect with AC voltage is better when compared to DC voltage.

Also, the consumed energy in the case of DC voltage is found to be higher than that consumed

when AC voltage is applied, and this is because of the Joule effect. Also, it has been observed that

the higher the amount of water used in the preparation of the sample, the lower the electrothermal

effect obtained; this is related to the higher porosity obtained and, hence, the higher electrical

resistance achieved.

285

286

287

288

289

290

291

292

293

294

295

296

297

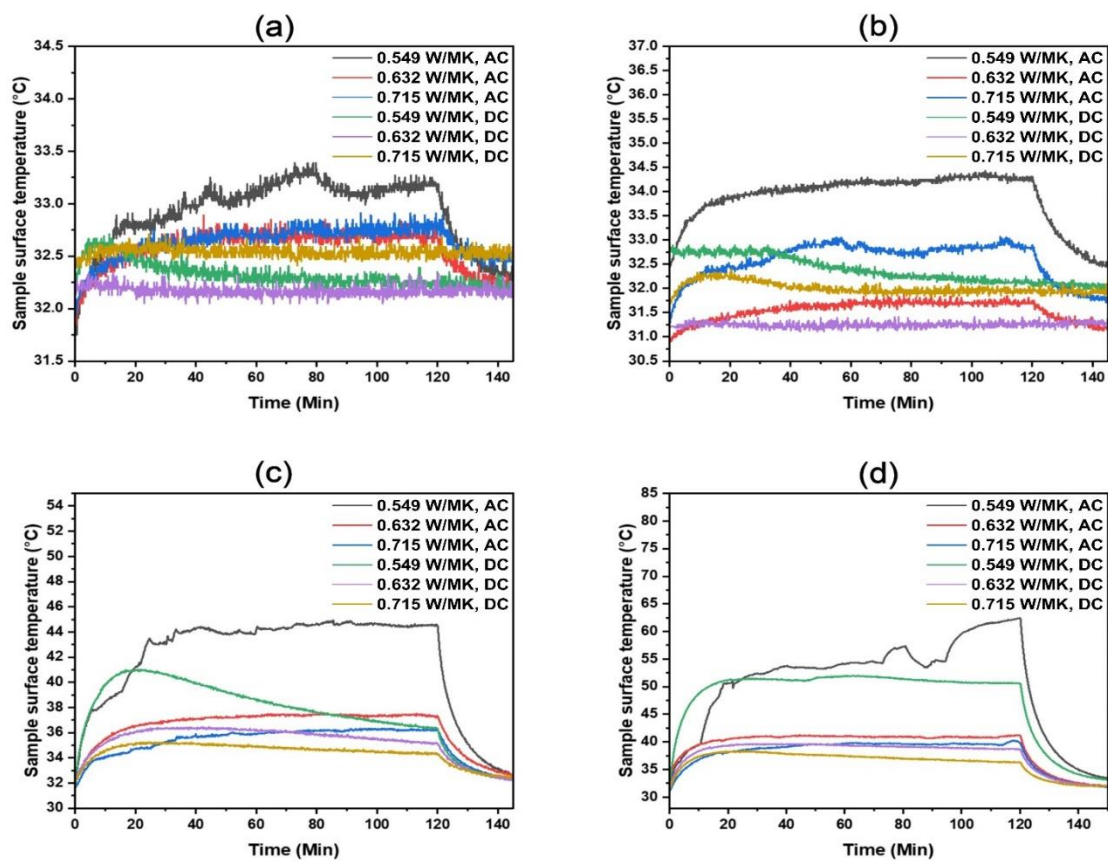
298

299

300

301 An important issue was noticed regarding the stability of the electrothermal performance of the  
302 samples. It has been observed that the samples gradually lose their ability to convert the electrical  
303 field into heat. The rate at which this happens depends on the type of the applied voltage; the AC  
304 voltage reduces that rate lower than the DC voltage. This indicates that something is changed in  
305 the electric circuit when the electric field is applied. Keep in mind that the mechanisms of electrical  
306 conduction in geopolymer depend either on the movement of sodium or potassium ions, the  
307 movement of free electrons, or the movement of hydroxide ions resulting from the water content  
308 when an electric field is applied [42–44]. Two possible reasons can explain this: the first is the  
309 increase of the electrical resistance due to the destruction of the conductive paths, and the second  
310 is the generation of a barrier between the sample and the electrode. Zhang et al. claimed that the  
311 decrease in the electrothermal effect of a sample containing 100 w.t% graphite, whose  
312 electrothermal performance was tested at 7 days, is due to the first reason: they suggested that the  
313 evaporation of water during the heating cycle leads to a shrinkage of the gel in the geopolymer  
314 and, consequently, to a destruction of the conduction network [45]. However, such a scenario may  
315 be accepted for the samples at an early age, when the polymerization process is going on and its  
316 byproduct, water, is formed. Nevertheless, that scenario is less probable when the sample is tested  
317 after the age of 28 days.

318 In the current study, it has been found that a barrier layer is formed between the copper electrode  
319 and the sample surface, as shown in Figure 12; after removing this layer via polishing, the circuit  
320 restored its electrothermal performance. The presence of this layer suggests that there are mobile  
321 ions in the sample that can be drifted via the electric field and react with the copper electrode to  
322 form that layer. The presence of such ions in the geopolymer was proved by Cui et al. [46].



323  
 324 **FIGURE 11** The electrothermal effect of geopolymer samples (a) GP-1; (b) GP-2; (c) GP-3;  
 325 (d) GP-4



326  
 327 **FIGURE 12** The barrier layer formed between the electrode and the sample

328  
 329 In order to support this scenario, the electrothermal behavior was evaluated after immersing the  
 330 samples in deionized water for 24 hours to remove the free ions and drying them at 100°C for 3  
 331 hours. **Figure 13** illustrates the electrothermal behavior of the chosen samples over three cycles;

332 it can be seen that the electrothermal behavior of the sample is noticeably stable over the three  
333 cycles; this confirms that the formation of the barrier layer is the reason behind the loss of the  
334 electrothermal behavior of the samples. It should be noted that the electrical resistance of samples  
335 GP3-A and GP-4A decreased after removing the free ions to become 141.5 and 23.4 ohms,  
336 respectively, and a temperature of 58 and 142°C could be achieved using 12 and 9V DC. This  
337 electrothermal performance is superior as compared to that reported in the literature [19,28,45].

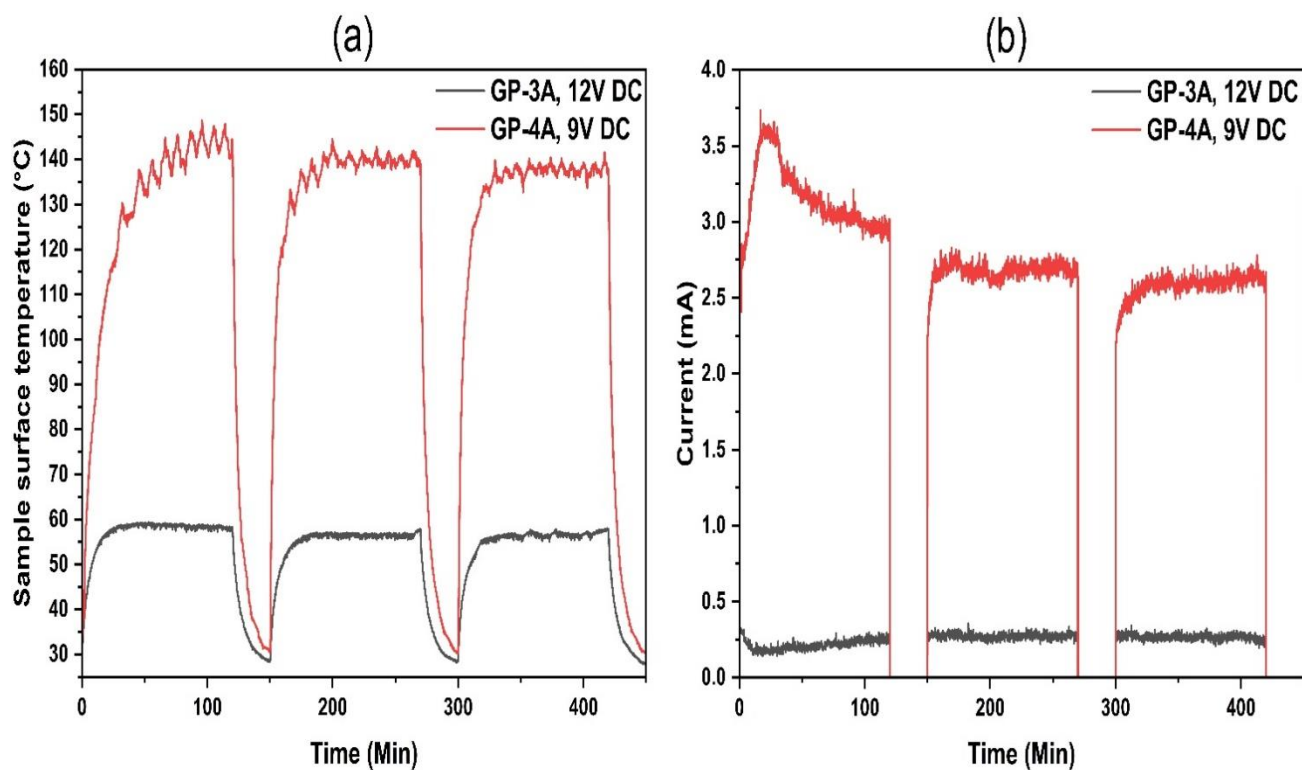
338

#### 339 **4. Conclusion**

340 The current study aimed to study the effect of adding carbon black to the metakaolin-based  
341 geopolymer. The following conclusions can be driven:

- 342 1- With the increase in the addition of carbon black, the compressive strength decreases and  
343 the electrical conductivity increases. However, using the right formula of the geopolymer  
344 along with the balance between the carbon black percent and the lowest water content  
345 possible, a conductive geopolymer with high compressive strength can be obtained.
- 346 2- The electrothermal performance of conductive geopolymer samples can be improved by  
347 increasing the percent of the carbon black and lowering the water content. However,  
348 increasing the addition percent increases energy consumption; thus, a compromise is  
349 needed between the desired temperature and the energy consumption. Additionally, the  
350 electrothermal performance is better with AC voltage compared to DC voltage applied.

351 The reason for the deterioration of the electrothermal performance is the formation of a barrier  
352 layer between the electrode and the sample surface. This can be avoided by removing the free ions  
353 from the sample via washing.



35.  
 355 **FIGURE 13** (a) electrothermal behavior and (b) energy consumption of GP-3A, GP-4A after  
 356 removing the free ions

357  
 358 **5. Recommendation**

359 It is recommended to carefully evaluate the homogeneity of the composite geopolymer and  
 360 to perform measurements of the compressive strength, electrical performance and  
 361 electrothermal performance of the homogeneous geopolymer well to ensure the reliability  
 362 of performance assessment.

363  
 364 **6. Reference**

365 [1] Jwaida Z, Dulaimi A, Mashaan N, Othuman Mydin MA. "Geopolymers: The green  
 366 alternative to traditional materials for engineering applications". Infrastructures (Basel).  
 367 2023, 8–98.

368 [2] Bai C, Colombo P. "Processing, properties and applications of highly porous geopolymers: A  
 369 review". Ceram Int. 2018, 44, 16103–18.

- 370 [3] Duan P, Yan C, Zhou W, Luo W, Shen C. "An investigation of the microstructure and  
371 durability of a fluidized bed fly ash–metakaolin geopolymer after heat and acid exposure".  
372 Mater Des. 2015, 74, 125–37.
- 373 [4] Hassan A, Arif M, Shariq M. "A review of properties and behaviour of reinforced  
374 geopolymer concrete structural elements-A clean technology option for sustainable  
375 development". J Clean Prod. 2020, 245–118762.
- 376 [5] de Toledo Pereira DS, da Silva FJ, Porto ABR, Candido VS, da Silva ACR, Garcia Filho  
377 FDC, Monteiro SN. "Comparative analysis between properties and microstructures of  
378 geopolymeric concrete and portland concrete". Journal of Materials Research and  
379 Technology. 2018, 7, 606–11.
- 380 [6] Karthik A, Sudalaimani K, Vijayakumar CT. "Durability study on coal fly ash-blast furnace  
381 slag geopolymer concretes with bio-additives". Ceram Int. 2017, 43, 11935–43.
- 382 [7] Turner LK, Collins FG. "Carbon dioxide equivalent (CO<sub>2</sub>-e) emissions: A comparison  
383 between geopolymer and OPC cement concrete". Constr Build Mater. 2013, 43, 125–30.
- 384 [8] Paruthi S, Husain A, Alam P, Khan AH, Hasan MA, Magbool HM. "A review on material mix  
385 proportion and strength influence parameters of geopolymer concrete: Application of ANN  
386 model for GPC strength prediction". Constr Build Mater. 2022, 356–129253.
- 387 [9] Taki K, Mukherjee S, Patel AK, Kumar M. "Reappraisal review on geopolymer: A new era  
388 of aluminosilicate binder for metal immobilization". Environ Nanotechnol Monit Manag.  
389 2020, 14–100345.
- 390 [10] Tan TH, Mo KH, Ling T-C, Lai SH. "Current development of geopolymer as alternative  
391 adsorbent for heavy metal removal". Environ Technol Innov. 2020, 18–100684.
- 392 [11] He P, Cui J, Wang M, Fu S, Yang H, Sun C, Duan X, Yang Z, Jia D, Zhou Y. "Interplay  
393 between storage temperature, medium and leaching kinetics of hazardous wastes in  
394 Metakaolin-based geopolymer". J Hazard Mater. 2020, 384–121377.
- 395 [12] Jiang C, Wang A, Bao X, Ni T, Ling J. "A review on geopolymer in potential coating  
396 application: Materials, preparation and basic properties". Journal of Building Engineering.  
397 2020, 32–101734.
- 398 [13] Lahoti M, Tan KH, Yang E-H. "A critical review of geopolymer properties for structural  
399 fire-resistance applications". Constr Build Mater. 2019, 221, 514–26.

- 400 [14] Davidovits J. "Geopolymers: Ceramic-like inorganic polymers". *J Ceram Sci Technol*.  
401 2017, 8, 335–50.
- 402 [15] Dai S, Wang H, An S, Yuan L. "Mechanical properties and microstructural characterization of  
403 metakaolin geopolymers based on orthogonal tests". *Materials*. 2022, 15–2957.
- 404 [16] Rashad AM. "A comprehensive overview about the influence of different additives on the  
405 properties of alkali-activated slag—A guide for Civil Engineer". *Constr Build Mater*. 2013,  
406 47, 29–55.
- 407 [17] Rashad AM. "Alkali-activated metakaolin: A short guide for civil Engineer—An overview".  
408 *Constr Build Mater*. 2013, 41, 751–65.
- 409 [18] Irshidat MR, Al-Nuaimi N, Rabie M. "Sustainable utilization of waste carbon black in  
410 alkali-activated mortar production". *Case Studies in Construction Materials*. 2021, 15–  
411 e00743.
- 412 [19] Fiala L, Petříková M, Lin W-T, Podolka L, Černý R. "Self-heating ability of geopolymers  
413 enhanced by carbon black admixtures at different voltage loads". *Energies (Basel)*. 2019, 12–  
414 4121.
- 415 [20] Vlachakis C, Wang X, Al-Tabbaa A. "Investigation of the compressive self-sensing  
416 response of filler-free metakaolin geopolymer binders and coatings". *Constr Build Mater*.  
417 2023, 392–131682.
- 418 [21] Mizerová C, Kusák I, Rovnaník P, Bayer P. "Metakaolin/carbon black geopolymer with  
419 enhanced electrical properties". *IOP Conf Ser Mater Sci Eng*. vol. 549, IOP Publishing,  
420 2019, p. 012033.
- 421 [22] Mizerová C, Kusák I, Rovnaník P. "Application of carbon black in conductive fly ash  
422 geopolymer mortars". *IOP Conf Ser Mater Sci Eng*. vol. 583, IOP Publishing, 2019, p.  
423 012014.
- 424 [23] Arif FT, Heryanto H, Sulieman A, Bradley DA, Tahir D. "Geopolymer cellulose-based  
425 composite Black Carbon (BC)/Fe/Cu/polyvinyl alcohol for eco-friendly apron X-ray".  
426 *Radiation Physics and Chemistry*. 2023, 207–110843.
- 427 [24] Rauf N, Darmawan ZT, Ilyas S, Heryanto H, Fahri AN, Rahmat R, Abdullah B, Tahir D. "Effect  
428 of Fe<sub>3</sub>O<sub>4</sub> in enhancement optical and gamma ray absorption properties of geopolymer apron  
429 cassava starch/black carbon/glycerin". *Opt Mater (Amst)*. 2021, 113–110887.
- 430 [25] Gu G, Ma T, Chen F, Han C, Li H, Xu F. "Co-modifying geopolymer composite by nano  
431 carbon black and carbon fibers to reduce CO<sub>2</sub> emissions in airport pavement induction  
432 heating". *Compos Part A Appl Sci Manuf*. 2024, 177–107951.

- 433 [26] Han J, Pan J, Wang X, Cai J, Gu L, Yang J. "Conductive behavior of engineered geopolymer  
434 composite with addition of carbon fiber and nano-carbon black". *Ceram Int.* 2023, 49, 32035–  
435 48.
- 436 [27] Mizerová C, Kusák I, Topolář L, Schmid P, Rovnaník P. "Self-sensing properties of fly ash  
437 geopolymer doped with carbon black under compression". *Materials.* 2021, 14–4350.
- 438 [28] Cai J, Li X, Tan J, Vandevyvere B. "Fly ash-based geopolymer with self-heating capacity  
439 for accelerated curing". *J Clean Prod.* 2020, 261–121119.
- 440 [29] Wardhono A, Law DW, Molyneaux TCK. "Strength of alkali activated slag and fly ash-  
441 based geopolymer mortar". *Proceedings of Microstructural-Related Durability of*  
442 *Cementitious Composites, Microdurability.* 2012.
- 443 [30] Alnasur MSH, Al-hydary IAD. "Development of Lightweight Geopolymer Concrete:  
444 Strength and Density Studied". *Journal of University of Babylon for Engineering Sciences.*  
445 2023, 31, 15–25.
- 446 [31] Mizerová C, Kusák I, Rovnaník P. "Electrical properties of fly ash geopolymer composites  
447 with graphite conductive admixtures". *Acta Polytech CTU Proc.* 2019, 22, 72–6.
- 448 [32] Hotěk P, Fiala L, Černý R. "Thermoelectric properties of metashale geopolymer mortar  
449 doped with graphite powder". *J Phys Conf Ser.* vol. 2628, IOP Publishing. 2023, p. 012006.
- 450 [33] Dubyey L, Ukrainczyk N, Yadav S, Izadifar M, Schneider JJ, Koenders E. "Carbon  
451 nanotubes and nanohorns in geopolymers: A study on chemical, physical and mechanical  
452 properties". *Mater Des.* 2024, 240–112851.
- 453 [34] Agustini NKA, Triwiyono A, Sulisty D. "Effects of water to solid ratio on thermal  
454 conductivity of fly ash-based geopolymer paste". *IOP Conf Ser Earth Environ Sci.* vol. 426,  
455 IOP Publishing. 2020, p. 012010.
- 456 [35] Zhang Y, He P, Yuan J, Yang C, Jia D, Zhou Y. "Effects of graphite on the mechanical and  
457 microwave absorption properties of geopolymer based composites". *Ceram Int.* 2017, 43,  
458 2325–32.
- 459 [36] Kuenzel C, Vandeperre LJ, Donatello S, Boccaccini AR, Cheeseman C. "Ambient  
460 temperature drying shrinkage and cracking in metakaolin-based geopolymers". *Journal of*  
461 *the American Ceramic Society.* 2012, 95, 3270–7.

- 462 [37] Li Y, Zhang W, Zhao J, Li W, Wang B, Yang Y, Sun J, Fang X, Xia R, Liu Y. "A route of  
463 alkylated carbon black with hydrophobicity, high dispersibility and efficient thermal  
464 conductivity". *Appl Surf Sci.* 2021, 538–147858.
- 465 [38] Zhang D, Zhu H, Wu Q, Yang T, Yin Z, Tian L. "Investigation of the hydrophobicity and  
466 microstructure of fly ash-slag geopolymer modified by polydimethylsiloxane". *Constr  
467 Build Mater.* 2023, 369–130540.
- 468 [39] Lasia A. *Electrochemical Impedance Spectroscopy and its Applications.* Springer. New  
469 York, 2014.
- 470 [40] Payakaniti P, Pinitsoontorn S, Thongbai P, Amornkitbamrung V, Chindaprasirt P.  
471 "Electrical conductivity and compressive strength of carbon fiber reinforced fly ash  
472 geopolymeric composites". *Constr Build Mater.* 2017, 135, 164–76.
- 473 [41] Zhang S, Ukrainczyk N, Zaoui A, Koenders E. "Electrical conductivity of geopolymer-  
474 graphite composites: Percolation, mesostructure and analytical modeling". *Constr Build  
475 Mater.* 2024, 411–134536.
- 476 [42] Cai J, Pan J, Li X, Tan J, Li J. "Electrical resistivity of fly ash and metakaolin based  
477 geopolymers". *Constr Build Mater.* 2020, 234–117868.
- 478 [43] Zhang Y, Chen S, Liang T, Ruan S, Wang W, Lin J, Liu Y, Yan D. "EIS investigation on  
479 electrical properties of metakaolin-based geopolymer". *Constr Build Mater.* 2024, 437–  
480 136851.
- 481 [44] Sellami M, Barre M, Toumi M. "Synthesis, thermal properties and electrical conductivity  
482 of phosphoric acid-based geopolymer with metakaolin". *Appl Clay Sci.* 2019, 180–105192.
- 483 [45] Zhang Y, Lin J, Chen S, Ruan S, Wang W, Liu Y, Yan D. "Electrothermal effect of carbon  
484 fiber and graphite reinforced metakaolin-based geopolymer". *Int J Appl Ceram Technol.*  
485 2024.
- 486 [46] Cui X-M, Zheng G-J, Han Y-C, Su F, Zhou J. "A study on electrical conductivity of  
487 chemosynthetic Al<sub>2</sub>O<sub>3</sub>–2SiO<sub>2</sub> geopolymer materials". *J Power Sources.* 2008, 184, 652–6.  
488